STM JOURNALS

Journal of
Polymer & Composites

ISSN: 2321-2810 (Online)
ISSN: 2321-8525 (Print)
Volume 13, Special Issue 1, 2025
DOI (Journal): 10.37591/JoPC

https://journals.stmjournals.com/jopc

Research JoPC

Investigation of Electronic Transport Characteristics of Co-Doped B40 Molecular Junction for Detection of Isoprene: A DFT Study

Jaskaran Singh Phull[1], Harmandar Kaur[2,*], Manjit Singh[3], Butta Singh[4], Himali Sarangal[5]

Abstract

The early identification of lung cancer is crucial and it can be diagnosed non-invasively by assessing the exhalation. Analysing a patient's breath profile can reveal malignant growths in their lungs. In this work, B_{40} co-doped with indium and iron is used as a molecular junction to sense isoprene, a well-known lung cancer biomarker present in the exhalation. The electronic transport characteristics of the molecular junction designed for isoprene detection are assessed. Using density functional theory, an extensive investigation is conducted in order to analyse the electronic transport properties, such as the density of states and the transmission spectrum for both equilibrium and non-equilibrium conditions of the designed junction to ascertain its ability to detect isoprene. Additionally, the non-equilibrium Green's function (NEGF) formalism is used to study the transport parameters, such as electrostatic difference potential, conductance and IV characteristics, for the isoprene co-doped B_{40} molecular junction. Investigation reveals that isoprene in the scattering region improves transmission across the junction and, as a result, raises the conductivity of the co-doped B_{40} molecular junction. Also, the electronic characteristics investigation shows that the main pathways of transmission in the co-doped B_{40}-isoprene molecular junction are the lowest unoccupied molecular orbitals. The electrostatic difference potential reveals the prevalence of potential difference across the junction leading to ease of conduction. The results of IV analysis show the presence of negative-differential resistance behaviour in the junction.

Keywords: DFT, sensing, borospherene, molecular junction, B40

INTRODUCTION

***Author for Correspondence**
Harmandar Kaur

[1]Student, Department of Engineering & Technology, GNDU Regional Campus Jalandhar Punjab India
[2]Assistant Professor, Department of Engineering & Technology, GNDU Regional Campus Jalandhar Punjab India
[3]Assistant, Professor, Department of Engineering & Technology, GNDU Regional Campus Jalandhar Punjab India
[4]Associate Professor, Department of Engineering & Technology, GNDU Regional Campus Jalandhar Punjab India
[5]Assistant Professor, Department of Engineering & Technology, GNDU Regional Campus Jalandhar Punjab India

Received Date: April 23, 2024
Accepted Date: May 14, 2024
Published Date: December 10, 2024

Citation: Jaskaran Singh Phull, Harmandar Kaur, Manjit Singh, Butta Singh, Himali Sarangal. Investigation of Electronic Transport Characteristics of co-doped B40 Molecular Junction for Detection of Isoprene: A DFT Study. Journal of Polymer & Composites. 2025; 13(Special Issue 1): S907–S916p.

In the periodic table, boron and carbon reside adjacent to each other [1]. Numerous structural models, such as nanosheets, nanotubes, and nanocages, have been investigated owing to the unique characteristics [2]. Given its inherent characteristics, such as its high melting point, light weight, and conductivity, boron nanoclusters have been studied for an array of applications. Several size variants of boron fullerenes have been the focus of substantial theoretical and experimental research since the 2007 discovery of B_{80} via ab initio calculations [3]. The discovery of C_{60} has prompted more research into related structures. In response to the 2014 discovery of all-boron fullerene (B_{40}), which has been backed by both theoretical and experimental studies [4-5]. various kinds of boron structures, including boranes, polyhedral boranes, and their derivatives, as well as

© STM Journals 2025. All Rights Reserved

boron nanoclusters, have been sought after. The density functional theory (DFT) approach has been used to study the absorption of CO_2 by borospherene [6-7]. Using B_{40} and Li@B_{40}, the DFT method for NO_2 detection has been investigated [8–12]. B_{40} fullerene is co-doped wherein multiple dopants can be simultaneously added (here we have dopants: Fe and In). With the addition of appropriate dopants, the electronic transport characteristics of B40 fullerene can be improved [13]. This work investigates the use of co-doped B_{40} fullerene for molecular junction sensing of isoprene, the most well-known lung cancer biomarker accessible via exhalation. By using density functional theory and the non-equilibrium Green's function (NEGF), the electronic transport parameters, such as the density of states, transmission spectra, electrostatic difference potential, conductance and current-voltage (I-V) characteristics are calculated and analysed for detection of isoprene by co-doped B40 molecular junction.

METHODOLOGY

There are two six-membered rings and four seven-membered rings on the surface of the B_{40} nanocage. The co-doped B_{40} molecular junction device is being investigated in an attempt to detect prominent lung cancer indicator i.e. isoprene. The left electrode, right electrode, and scattering region with co-doped B_{40} form a molecular junction that includes the two-probe model under investigation, as seen in Figure 1. Since gold is fairly stable at room temperature, it is typically chosen as the electrode material. The molecular junction device shown in Fig.1 has the lung cancer VOC i.e. isoprene located in the scattering zone.

COMPUTATIONAL METHOD

To take into account the characteristics of electronic transport, a two-probe model with left electrode, right electrode, and scattering zone is assimilated. The co-doped B_{40}-isoprene complex is placed in the scattering zone of the two-probe model between the gold electrodes to investigate the electronic transport characteristics. DFT is used for the electronic transport simulations, which are included in the Atomistix Toolkit's Virtual Nanolab [14]. The exchange correlation functional has been characterised for computing and optimisation using the spin unpolarized generalised gradient approximation of Perdew-Burke-Ernzerhof [15]. with double-zeta polarised basis set.

Both the local and gradient values of the electron density are employed in the generalised gradient approximation. The electronic transport characteristics of the co-doped B_{40}molecular junction were investigated using the DFT-PBE method in several previous investigations [16–17].

A popular method for modelling molecular junctions is the DFT-NEGF regime. Essentially, this method operates as follows: the density matrix is comprehended by applying the energy integrals of Green's function; (2) the electron density and density of states (DOS) are then computed; and (3) the transmission function is then found by applying the following equation:

$$T(E) = T_r[\Gamma_L(E)\, G(E)\, \Gamma_R(E)\, G^*(E)] \quad (1)$$

where Γ_L and Γ_R represent the coupling functions of the imaginary parts of self-energies of left and right electrodes respectively; G* (E) and G (E) denote the advanced and retarded values of Green's function. Post these calculations, the transport characteristics of the molecular junction can be calculated. Landauer-Buttiker formula is utilized to compute the value of current as follows:

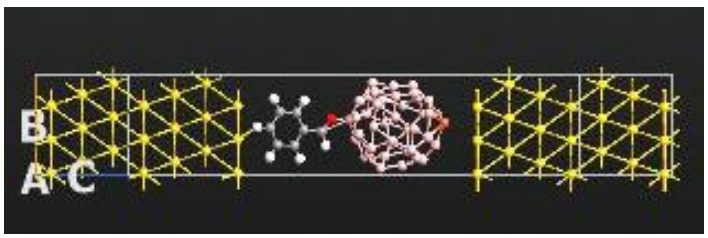

Figure1. Bulk structure of molecular junction comprising of co-doped B_{40} with isoprene (yellow: gold, white:hydrogen, grey:carbon, pink: boron).

© STM Journals 2025. All Rights Reserved

$$I = \frac{e}{h}\int T(E)[\int\left(\frac{E-E_F^L+eV_R}{k_BT_R}\right) - \int\left(\frac{E-E_F^L+eV_L}{k_BT_L}\right)]\mathrm{dE} \quad (2)$$

Here, E_F^Lrepresents Fermi energy, ∫ denotes Fermi function, and $T_{L/R}$ represents temperatures of left/right electrodes; T (E) denotes the coefficient of transmission.

RESULTS AND DISCUSSION

We investigate the equilibrium state of the electronic transport properties of the co-doped B_{40} molecular junction with the volatile organic chemical i.e. isoprene. Moreover, with a bias between 0V and 2V, the electronic transport parameters of the non-equilibrium state [18] are examined.

Conductance, I-V curves, density of states, electrostatic difference potential and transmission spectra are among the computation outcomes. The density of states presents the quantum states that participate in the transmission process. It also provides essential information on the interactions between the adsorbent and adsorbate and depicts the arrangement of the molecular orbitals. The transmission spectrum study demonstrates the main chemical orbitals that are responsible for transmission.

Density of States Analysis

The aspects of the transport process are explicitly described by DOS by presenting the quantum states involved in the transmission process from PBE-DFT parameterization. It facilitates the analysis of the quantum states that are found close to the Fermi level.

The broader peak shown in Figure 2 residing throughout the energy range implies that there is greater interaction between central molecule and metallic electrodes. Hence, indicating strong coupling and easier transmission. The E_{HOMO} is -0.12eV and E_{LUMO} is 0.48eV as per the results obtained from the DOS analysis. This indicates an energy gap of 0.60eV is prevalent near the Fermi level.

Higher peaks are observed only on one side of the Fermi level that contributes to the transmission. Thus, the conductivity in isoprene-B_{40}molecular junction indicates that the co-doped B_{40}junction and isoprene are better interacting.

Transmission Spectrum Analysis

The transmission spectrum reveals the energy associated to the maximum electron transfer. First, the co-doped B_{40} molecular junction transmission spectrum assimilation is estimated at zero bias using isoprene in the scattering region. The results of the transmission spectrum analysis for the equilibrium state are shown in Figure3.

The energy levels at which the transmission process takes place correlate to the energy values at which the transmission peaks. Figure 3. demonstrates the presence of the transmission states at the equilibrium condition. The main transmission peaks with high transmission strength are present above the Fermi energy level, as seen in Figure 3. These are an indicative of the contribution from the lowest unoccupied molecular orbitals (LUMO) in the transmission process. As opposed to B_{40} molecular junction, the co-doped B_{40}-isoprene molecular junction shows greater transmission as is evident from Figure 3(b). This implies greater conduction.

Figure 4 presents the findings of the analysis of the transmission spectrum for the non-equilibrium state. It can be seen from the results of Figure 4(a)–4(k) that the transmission varies for external bias in the range of 0V to 2V.This analysis provides insights to the transmission process under the influence of applied bias. The bias is incremented in steps of 0.2Vand it is observed that the increase of the bias appends transmission states to the vicinity of the Fermi level mainly below the Fermi level. The transmission process is supported by the LUMO for the applied external bias.

© STM Journals 2025. All Rights Reserved

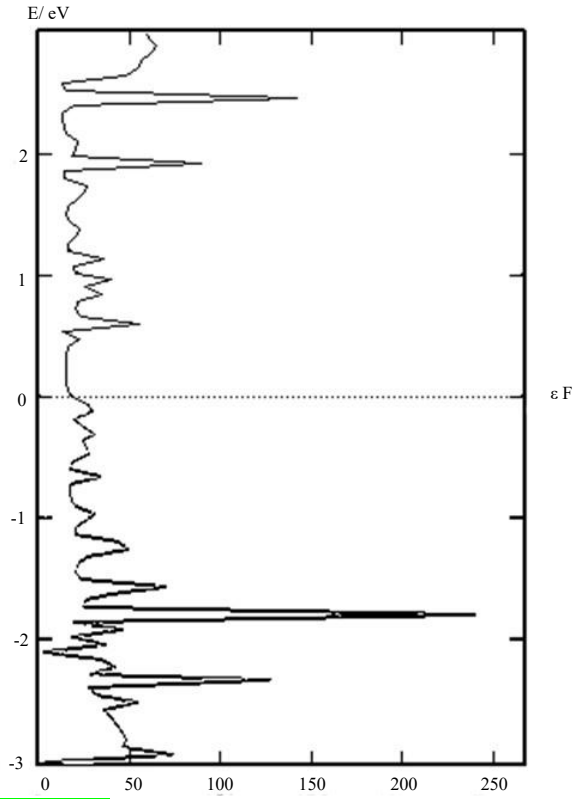

Figure 2. Density of states analysis of co-doped B_{40}-isoprene molecular junction.

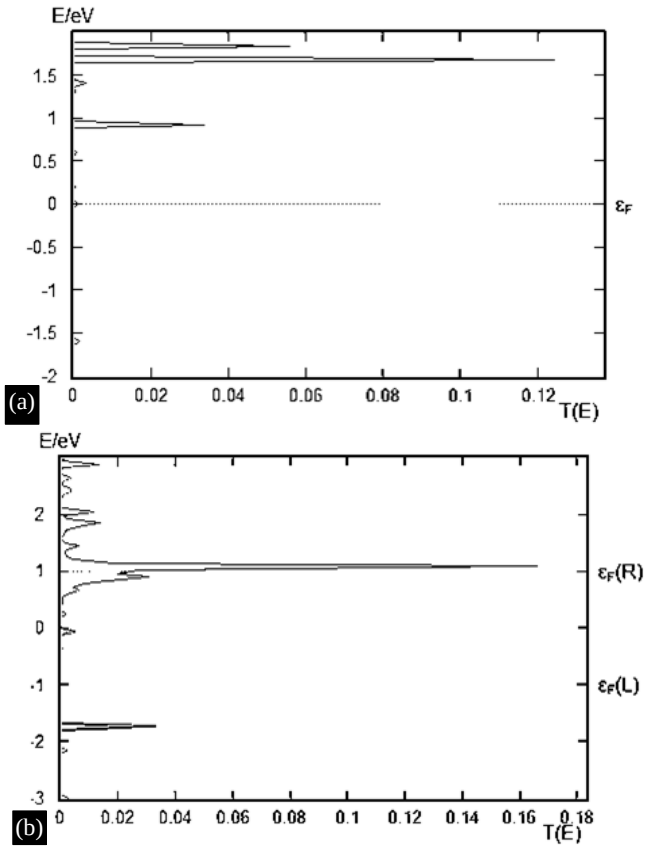

Figure 3. Transmission spectrum analysis of(a) B_{40} molecular junction (b) co-doped B_{40}-isoprene molecular junction for equilibrium condition.

© STM Journals 2025. All Rights Reserved

The total transmission spectra as is depicted in Figure 5, presents the overview of the transmission process throughout the energy range i.e. -2eV to 2eV. The analysis indicates the contribution by the LUMO with high transmission opposed to that of B40 molecular junction of Figure 5.

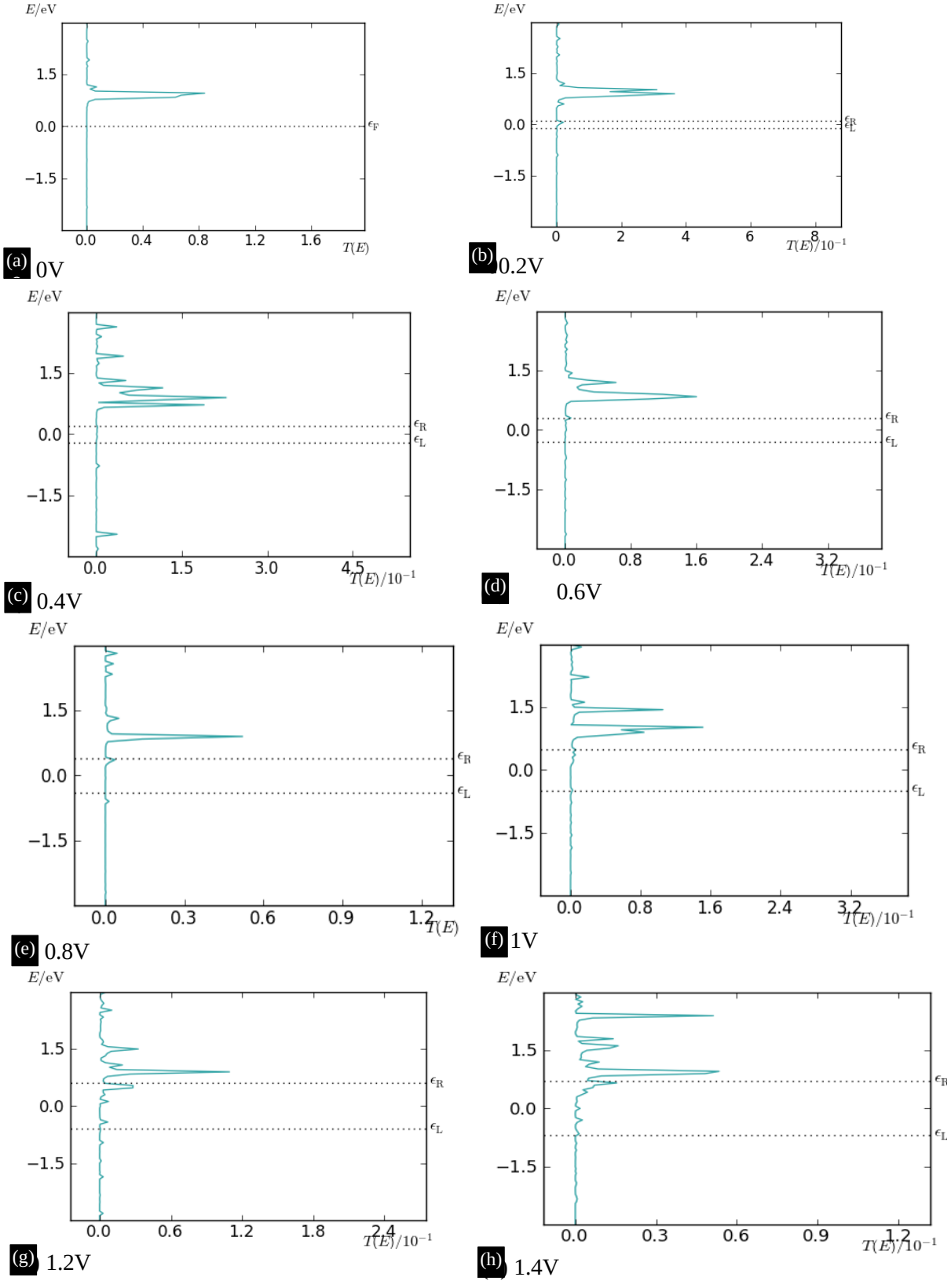

(a) 0V (b) 0.2V (c) 0.4V (d) 0.6V (e) 0.8V (f) 1V (g) 1.2V (h) 1.4V

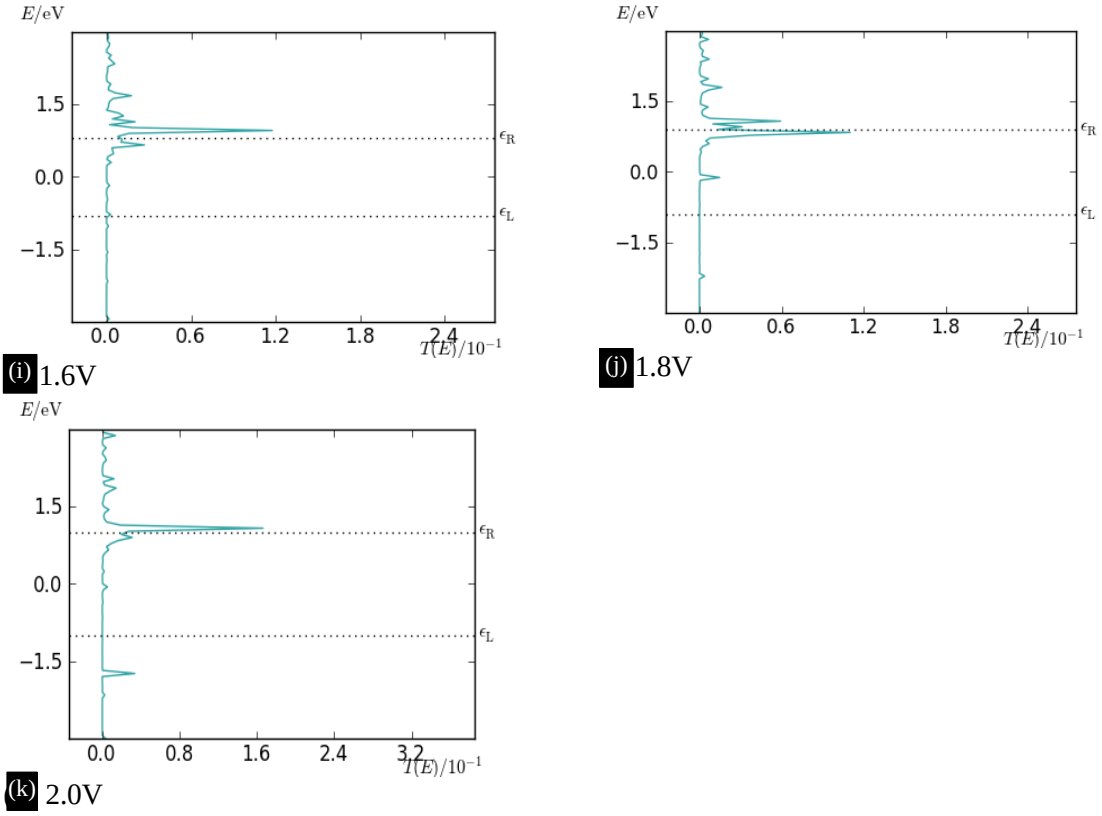

Figure 4. Transmission spectrum analysis of co-doped B_{40}-isoprene molecular junction for non-equilibrium condition.

Electrostatic Difference Potential

The electrostatic difference potential is computed self-consistently from the Kohn-Sham equations using DFT formalism. It is the difference in the potential between different states and configurations providing insights about the contributions of the atoms or molecules. It elucidates the binding assemblies and stability of the molecular assembly. The isosurface graphic shows the absolute value of the wave function. Figure 6 displays the electrostatic difference potential for the molecular junction considered an isovalue of 0.034.

Investigation of the electrostatic difference potential reveals that the variation in the reactivity, suggesting possible electron transmission from the left electrode to the right electrode. There exists a complete difference of potential in the left and right electrodes as is elucidated in Figure 6 indicating easy electron flow owing to potential difference suggesting the device's conduction is improved. Hence, the co-doped B_{40}molecular junction can be used for sensing of isoprene, a lung cancer VOC.

I-V Analysis

The IV characteristics, as determined using the non-equilibrium Green's function (NEGF) formalism, are displayed in Fig.7. The results present the variation of current for applied external bias ranging between 0 and 2 volts. First, NEGF computations are carried out, and the transmission coefficients are determined by applying the technique given in Eq. (3):

$$T(U) = tr(\mu_R F_C \mu_L F_C) \quad (3)$$

where, T(U) is the transmission coefficient, F_C is the Green's function, and is the imaginary part of self-energy for the left electrode if the L subscript is used, and the right electrode if the R subscript is used. Furthermore, the device's current I(V) is computed as follows:

$$I(V) = \frac{2e}{h} \sum_{\eta_L}^{\eta_R} (G(U - \eta_R) - G(U - \eta_L)T(U))\, dU \quad (4)$$

© STM Journals 2025. All Rights Reserved

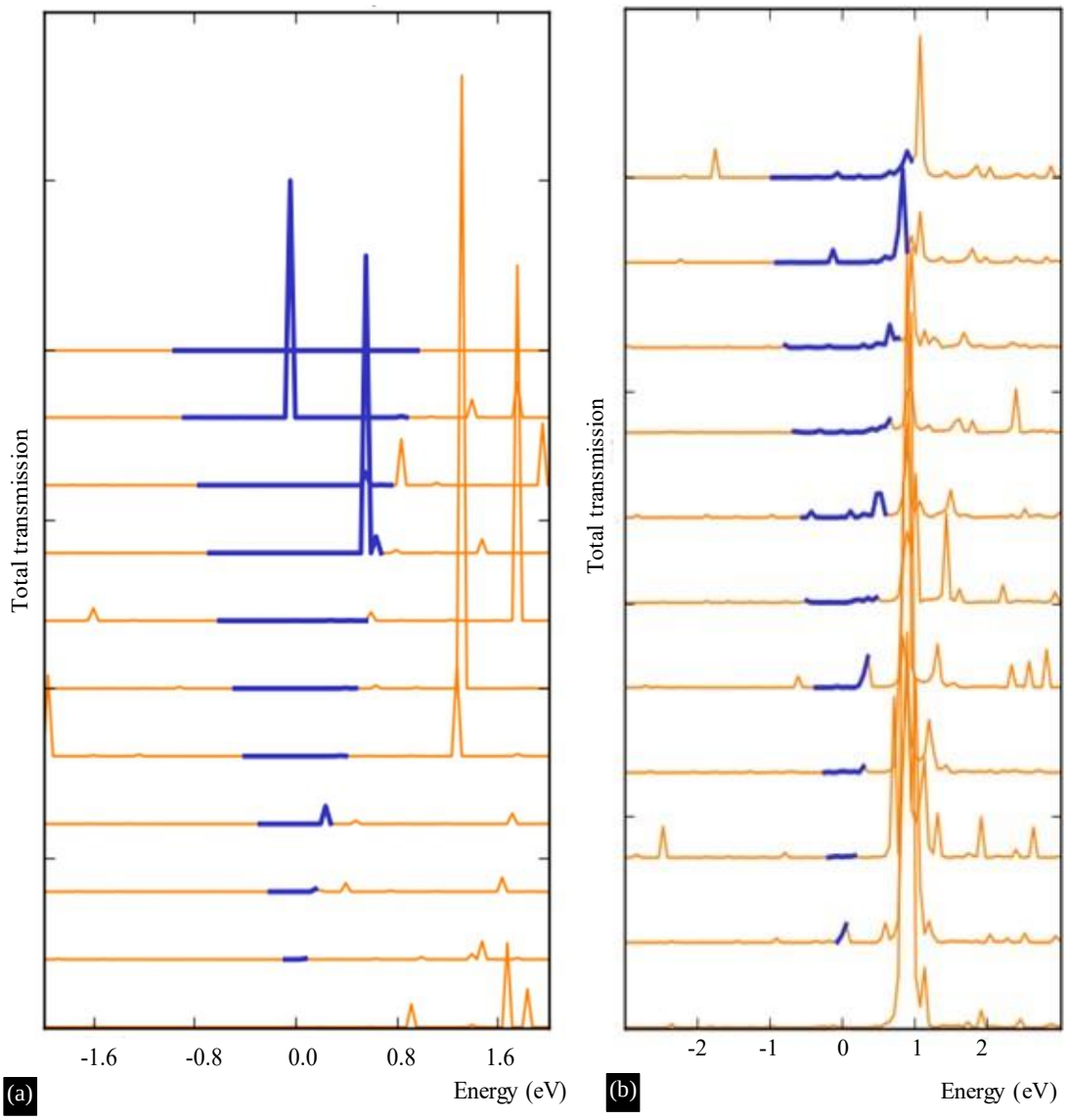

Figure 5. Total transmission spectrum analysis of (a) B_{40} molecular junction (b) co-doped B_{40}-isoprene molecular junction.

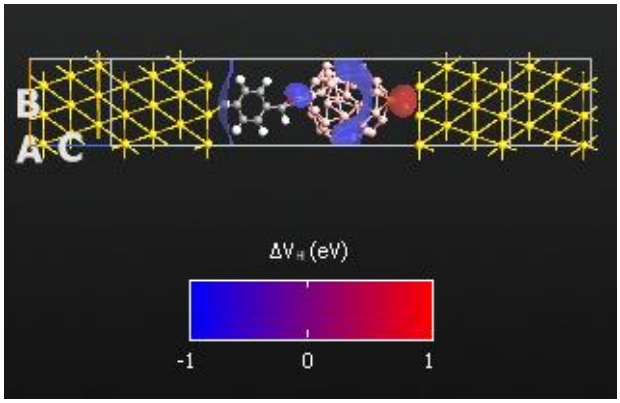

Figure 6. Electrostatic difference potentialof co-doped B_{40} on adsorption of isoprene.

where the chemical potentials of the electrode are denoted by $\eta_R$and η_L in this equation. For energy, U notation is used.The IV characteristics indicate the negative differential resistance prevails in the co-

© STM Journals 2025. All Rights Reserved

doped B_{40}-isoprene molecular junction. This signifies decrease in current with an increase in voltage indicating prevalence of negative differential behavior.

The conductance characteristics for the co-doped B_{40} molecular junction in presence of isoprene lung cancer VOC is shown in Figure 8. The analysis of the results obtained indicate the conductance and hence detection of isoprene by the co-doped B_{40} molecular junction.

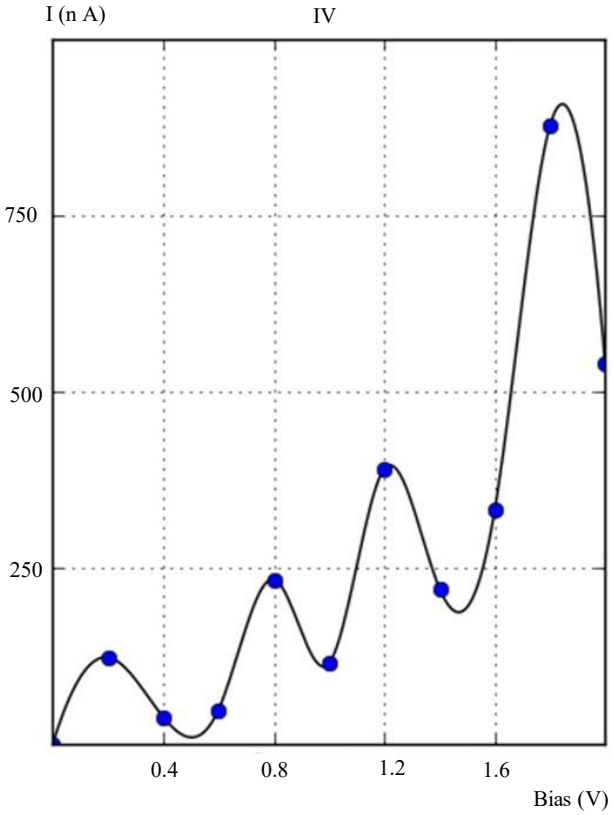

Figure 7. IV characteristics of co-doped B_{40}-isoprene molecular junction.

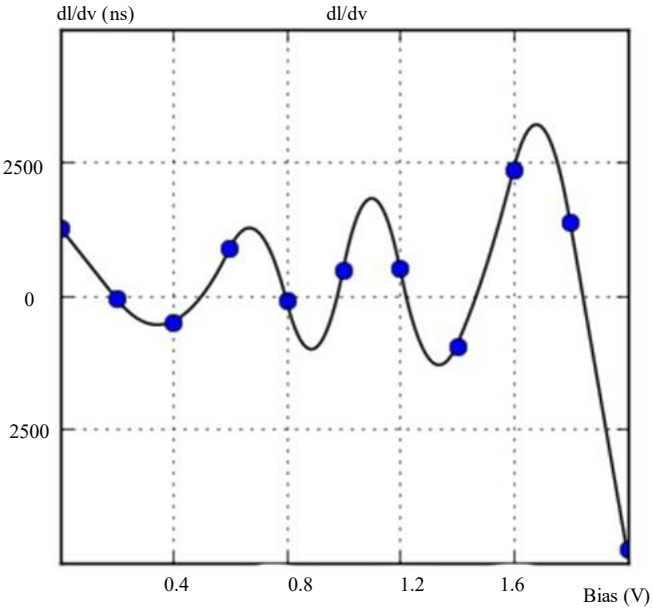

Figure 8. Conduction characteristics of co-doped B_{40}-isoprene molecular junction.

© STM Journals 2025. All Rights Reserved

CONCLUSION

Using density functional theory, the co-doped B_{40}as lung cancer biomarker is investigated. The detection of isoprene, a prominent volatile organic compound associated with lung cancer, is investigated by calculating the electronic and transport properties of the co-doped B_{40} molecular junction with isoprene in the scattering region. Investigations are conducted on the parameters, which include electrostatic difference potential, current-voltage characteristics, transmission spectra, conductance and density of states. Based on the investigations, it has been found that the lowest unoccupied molecular orbitals above the Fermi level contribute to the electron transmission process in the isoprene-B_{40} molecular device. Additionally, the results elucidate the detection of isoprene by the co-doped B_{40} molecular junction.

Acknowledgments

Funding

The authors declare that no funds, grants, or other support were received during the preparation of this manuscript.

Competing Interests

The authors have no relevant financial or non-financial interests to disclose.

Author Contributions

All authors contributed to the study conception and design. Material preparation, data collection and analysis were performed by Harmandar Kaur and Jaskaran Singh Phull. The first draft of the manuscript was written by Manjit Singh, Butta Singh , Himali Sarangal and Harmandar Kaur commented on previous versions of the manuscript. All authors read and approved the final manuscript.

REFERENCES

1. Novoselov KS, Geim AK, Morozov SV, et al. Electric Field Effect in Atomically Thin Carbon Films. *Science* 2004; 306 (5696): 666-9p.
2. Song X, Hu J, Zeng H. Two-dimensional Semiconductors: Recent Progress and Future Perspectives. *J. Mater. Chem. C* 2013; 1 (17): 2952-69p.
3. Szwacki NG, Sadrzadeh A, Yakobson BI, B_{80} fullerene: an ab initio prediction of geometry, stability, and electronic structure, *Phys. Rev. Lett*. 2007; 98 (166804). Erratum: *Phys. Rev. Lett.* 2008; 100 (159901).
4. Omidvar A. Dissociation of O_2 molecule on Fe/Nx clusters embedded in C_{60} fullerene, carbon nanotube and graphene, *Synth. Met*. 2017; 234: 38–46p.
5. Zhai H, Zhao Y, Li W et al. Observation of an all-boron fullerene. *Nat. Chem*. 2014; 6(8):727–31p.
6. G. Gao, F. Ma, Y. Jiao et al. Modelling CO_2 adsorption and separation on experimentally-realized B40 fullerene, *Comput. Mater. Sci.* 2015; 108(Part A): 38–41p.
7. Moradi M, Vahabi V, Bodaghi A. Computational study on the fullerene-like B_{40} borospherene properties and interaction with ammonia. *J. Mol. Liq*. 2016; 223, 315–20p. https://doi.org/10.1016/j.molliq.2016.07.147
8. Maniei Z, Shakerzadeh E, Mahdavifar Z. Theoretical approach into potential possibility of efficient NO_2 detection via B_{40} and Li@B_{40} fullerenes, *Chem. Phys. Lett.* 2018; 691: 360–65p.
9. Lin B, Dong H, Du C et al. B_{40} fullerene as a highly sensitive molecular device for NH_3 detection at low bias: a first-principles study. *Nanotechnology* 2016; 27(7): 075501. https://doi.org/10.1088/0957-4484/27/7/075501
10. Phull JS, Kaur H, Singh P et al. Investigation of Bulk, Electronic and Transport Properties of Armchair Silicene Nanoribbon as Liquefied Petroleum Gas Combustion Indicator: A DFT Study. In: Mehta, G., Wickramasinghe, N., Kakkar, D. (eds) Innovations in VLSI, Signal Processing and Computational Technologies. Lecture Notes in Electrical Engineering 1095. Singapore: Springer; 2024. https://doi.org/10.1007/978-981-99-7077-3_27

© STM Journals 2025. All Rights Reserved

11. Phull JS, Kaur H, Singh M et al. A First Principles Investigation of the Bulk and Electronic Properties of Doped Armchair Graphene Nanoribbon for Sensing Dimethyl Disulphide. Materials Science Forum. Trans Tech Publications Ltd; 2023. https://doi.org/10.4028/p-en9l10
12. Phull JS, Kaur H, Singh M et al. Investigation of the Bulk and Electronic Properties of Boron/Nitrogen/Indium Doped Armchair Graphene Nanoribbon for Sensing Plant VOC: A DFT Study. In: Saini, M.K., Goel, N., Shekhawat, H.S., Mauri, J.L., Singh, D. (eds) Agriculture-Centric Computation. Communications in Computer and Information Science, 1866. Springer; 2023. https://doi.org/10.1007/978-3-031-43605-5_18
13. Hamadi H, Shakerzadeh E, Mehdi DE. Exploring the potential use of Fe-decorated B_{40} borospherene as a prospective catalyst for oxidation of methane to methanol. *Journal of Molecular Graphics and Modelling* 2023; 118(108369). https://doi.org/10.1016/j.jmgm.2022.108369
14. Atomistic Toolkit Manual, Quantumwise Inc. Atomistix toolkit version 13.8.0, Quantumwise A/S. http://quantumwise.com
15. Perdew JP, Burke K, Ernzerhof M, Generalized gradient approximation made simple, *Phys. Rev. Lett*. 1996; 77:3865-68p.
16. Chen Q, Li WL, Zhao YF et al. Experimental and theoretical evidence of an axially chiral borospherene, *ACS Nano* 2015; 9(1):754-60p.
17. Tai TB, Nguyen MT. A new chiral boron cluster B_{44} containing nonagonal holes, *Chem. Commun.* 2016; 52:1653–6p.
18. Brandbyge M, Mozos JL, Ordejon P et al. Density-functional method for non equilibrium electron transport. *Phys. Rev. B* 2002; 65(165401) https://doi.org/10.1103/PhysR evB.65.165401

© STM Journals 2025. All Rights Reserved